

# **A sheath boundary condition for fast wave propagation near conducting surfaces**

**D. A. D'Ippolito and J. R. Myra**

*Lodestar Research Corporation,  
Boulder, Colorado, 80301*

November, 2011

*Submitted to Phys. Plasmas*

---

DOE/ER/54392-67 & DOE/ER/54823-13

LRC-11-147

---

***Lodestar Research Corporation***

*2400 Central Avenue #P-5*

*Boulder, CO 80301*

# A sheath boundary condition for fast wave propagation near conducting surfaces\*

D. A. D'Ippolito<sup>†</sup> and J. R. Myra

*Lodestar Research Corporation, 2400 Central Avenue, Boulder, Colorado 80301*

Radiofrequency (rf) waves can enhance electron losses to a material surface and generate rf sheath potentials which are significantly larger than the thermal Bohm sheath. The condition for this to occur is that the rf electric field has a component  $E_{\parallel}$  parallel to the equilibrium magnetic field. Thus, a proper treatment of rf wave propagation requires an accurate description of the geometry of the magnetic field and of the bounding surfaces, and a boundary condition (BC) that includes the effect on the waves of the electron-poor sheath. When the static magnetic field has a component at an angle to the sheath, the propagating fast wave (with  $E_{\parallel} = 0$ ) is coupled to a slow wave (with  $E_{\parallel} \neq 0$ ) in order to satisfy the boundary condition at the metal wall, and the time-averaged sheath potential has a strong component from rectification of the rf sheath. In this brief communication, a previously derived sheath BC is reformulated to treat the coupling of the fast wave to the slow wave analytically, thereby greatly reducing the necessary numerical resolution required for calculation of fast wave propagation.

PACS numbers: 52.35.Mw, 52.40.Fd, 52.40.Kh, 52.50.Qt, 52.55.Fa

<sup>†</sup>email: [dippolito@lodestar.com](mailto:dippolito@lodestar.com)

Previous theoretical and experimental work has shown that radio-frequency (rf) enhanced sheaths are an important feature in some regimes of fusion experiments using ion cyclotron resonance heating. The sheaths can lead to rf-specific impurity production, hot spots, edge power dissipation, and other effects which must be minimized for good performance, especially for the next generation of long-pulse tokamak experiments.. These issues have been discussed in a number of recent review and overview papers,<sup>1-3</sup> and continue to stimulate experimental work and modeling.<sup>4-9</sup> Antenna design activities, rf scenario development, and interpretation of experimental data, all require the development of rf wave codes which can self-consistently evaluate the effects of rf sheaths at the boundary. Previously, we have suggested one approach for developing self-consistent simulations, viz. the use of an “rf sheath” boundary condition (BC),<sup>10,11</sup> which treats the electron-poor sheath region as a thin vacuum layer. This vacuum layer approximation, employed previously in some codes as a sub-grid model,<sup>12</sup> captures the large change in the rf parallel electron response across the sheath interface.

This rf sheath BC is derived<sup>10,11</sup> using the continuity of the normal component of the displacement  $\mathbf{D} \equiv \epsilon \cdot \mathbf{E}$  and of the tangential components of the electric field  $\mathbf{E}$  across the plasma-vacuum (sheath) interface. The BC at this interface is given by

$$\mathbf{E}_t = \nabla_t (\Delta D_n / \epsilon_{sh}) , \quad (1)$$

where the subscripts n and t denote “normal” and “tangential” to the sheath surface, the field components are defined on the plasma side of the interface, and  $\Delta$  is the time-averaged sheath width (sufficient for computing the rectified sheath potential). We will refer to this BC as the “full sheath BC” to distinguish it from the reduced BC derived in this paper. The right hand side (rhs) contains the effect of the sheath capacitance ( $\propto 1/\Delta$ ). When the sheath capacitive impedance ( $\propto \Delta$ ) is neglected, one recovers the usual metal wall BC,  $\mathbf{E}_t = 0$ . Here,  $\epsilon_{sh}$  is the dielectric constant in the sheath region, and its vacuum value ( $\epsilon_{sh} = 1$ ) will be used here, unless otherwise noted.

If the sheath width  $\Delta$  is regarded as specified, Eq. (1) gives a linear relation between the rf fields and the rf sheath potential  $\Phi_{rf} \equiv \Delta \mathbf{E}_n^{(sh)} = \Delta D_n$ , where the

superscript (sh) indicates a field component on the vacuum side of the sheath-plasma interface. However, for self-consistency, the sheath width and the rf sheath potential have to satisfy the nonlinear Child-Langmuir (CL) law,<sup>13</sup>

$$\Delta = \lambda_d (e\Phi_{\text{sh}} / T_e)^{3/4}, \quad (2)$$

where  $\lambda_d = (T_e / 4\pi n e^2)^{1/2}$  is the electron Debye length and  $\Phi_{\text{sh}}$  is the rectified sheath potential defined subsequently [see Eq. ( )]. The CL constraint makes the BC nonlinear and can lead to multiple roots. Also note that the BC incorporates plasma dielectric effects through  $D_n \approx \mathbf{s} \cdot \mathbf{b} \epsilon_{\parallel} E_{\parallel}$ , where  $\mathbf{s}$  is the unit vector normal to the sheath. Only the waves with  $E_{\parallel} \neq 0$  make a significant contribution to the rhs of Eq. (1).

The rf  $E_{\parallel}$  component can be driven directly by an antenna or indirectly by coupling to another wave at the boundary. Except for special circumstances in the geometry (such as when the boundary is a flux surface) both wave polarizations are required to satisfy a general boundary condition such as Eq. (1), even in the metal wall limit. In tokamak geometry, this usually implies that the fast wave (FW) with  $E_{\parallel} = 0$  couples to the a slow wave (SW) with  $E_{\parallel} \neq 0$ . This SW  $E_{\parallel}$  increases the loss of electrons along the field lines and amplifies the sheath potential. In what follows, we will assume that the SW is evanescent near the wall where the BC is applied (see Fig. 1) (e.g. either due to the density regime or strong collisional absorption).

A number of model problems using the BC (1) have been solved analytically in simple one-dimensional geometry. The reader is referred to the introduction of Ref. 14 or to Appendix A in Ref. 15 for detailed summaries of this work, which illustrates the effects of the sheath capacitance on the rf fields and on sheath formation.

More recently, a new finite-element code<sup>16-18</sup> has been developed to calculate rf wave propagation in the scrape-off-layer (SOL) of a tokamak, including more realistic geometry of the magnetic field and of the material boundaries. The code incorporates the full sheath BC and computes the rf fields and the sheath formation self-consistently. The numerical calculations have shown that large-scale parallel computational resources are

required to carry out a simulation that treats both the ion scale ( $\sim \delta_i = c / \omega_{pi}$ ) for the FW, the electron scale ( $\sim \delta_e = c / \omega_{pe}$ ) for the SW, and the full sheath BC at the same time.

This problem motivates the present work. In this Brief Communication, we describe a reformulation of the sheath BC that allows the coupling of the FW to the SW to be treated analytically, so that only the ion scale needs to be resolved numerically. The basic idea is shown in Fig. 1. We consider the problem of a FW encountering a metal wall and assume that the plasma density is constant in a small region outside the sheath. The angle  $\theta$  between the  $\mathbf{B}$  field and the metal boundary is assumed to satisfy the inequality  $\theta > (m_e / m_i)^{1/2}$  to obtain an electron-poor sheath, which is the situation of interest here. We also assume the ordering

$$\lambda_d \ll \delta_e \ll \delta_i \quad (3)$$

where  $\lambda_d$  is the Debye length, and  $\delta_e, \delta_i$  are the electron and ion skin depths defined previously.

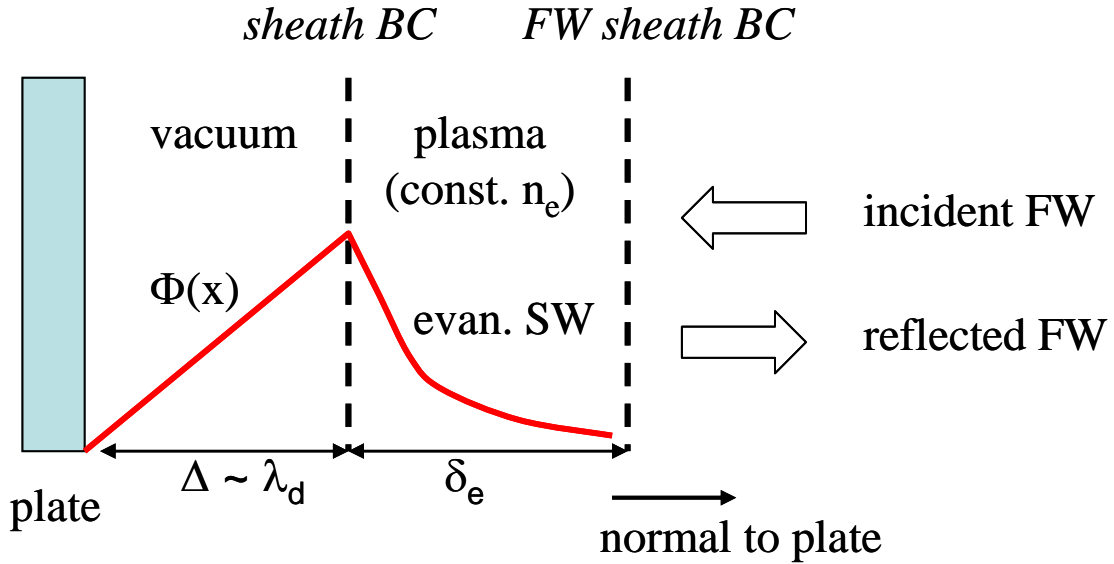


Fig. 1 Schematic of the sheath-plasma interface and two sheath BCs described in the text. The rf potential  $\Phi(x)$  increases linearly in the vacuum sheath region and then decays exponentially in the plasma region over the distance of an electron skin depth. The full sheath BC is applied at the sheath-plasma interface. When the SW is evanescent, an alternative approach is to apply the FW sheath BC at the beginning of the region where the SW is negligible.

The smallness of the Debye length, which is the typical scale of the sheath width, permits integrating over the sheath to obtain the original sheath BC.<sup>10,11</sup> In simulations using this BC, one does not have to resolve the sheath itself, but the SW must be resolved numerically in the plasma region just outside the sheath-plasma interface. In other words, the  $\lambda_d$  scale has been eliminated, but the  $\delta_e$  scale (of the SW) still needs to be resolved numerically. For problems involving FW propagation, we can go one step further and eliminate the  $\delta_e$  scale analytically, so that only the typical FW  $\delta_i$  scale needs to be resolved. As indicated in Fig. 1, this leads to a new BC which constrains only the FW. We will call this the “FW sheath BC,” which is the main result of this paper.

An example for which the new BC applies is the “far field sheath” problem<sup>10,19-22</sup> in which the FW propagates into a boundary and cannot satisfy the Maxwell BCs without coupling to a SW. This situation arises when the single pass absorption is low<sup>10,19,20</sup> or when the FW propagates nearly parallel to  $\mathbf{B}$  in the SOL.<sup>21-24</sup> The far field sheath problem has been addressed analytically in Ref. 19 in a one-dimensional (1D) model using the full sheath BC [Eq. (1)]. This earlier paper provides the starting point for our formulation of the new sheath BC for fast waves. The essential element for applicability of this model is not whether the sheaths are in the near-field or far-field, but that a FW is launched and is coupled to a strongly evanescent SW by the BC.

The sheath BC in Eq. (4) can be written in the form

$$\mathbf{s} \times \mathbf{E} = \mathbf{s} \times \nabla(\Delta D_n) \quad , \quad (4)$$

where all quantities are evaluated at the sheath-plasma interface,  $D_n \equiv \mathbf{s} \cdot \mathbf{D} = \mathbf{s} \cdot \boldsymbol{\epsilon} \cdot \mathbf{E}$ , and the boundary is *not* assumed to coincide with a magnetic flux surface ( $\mathbf{s} \cdot \mathbf{b} \neq 0$ ). When this last condition is satisfied, the incident FW will not satisfy either the conducting wall BC or sheath BC without coupling to additional waves.

Following Ref. 19, we consider a minimal three-wave coupling model, consisting of an incident and reflected FW and an evanescent SW, denoted by subscripts 0, 1 and 2 respectively. Thus, one can express the total rf electric field in Fourier space as

$$\mathbf{E} = e^{-i\omega t} e^{ik_y y} e^{ik_z z} \sum_{j=0}^2 E_j \mathbf{e}_j e^{ik_j x} . \quad (5)$$

where the vectors without carats,  $\mathbf{e}_j$  ( $j=0,1,2$ ), are the wave polarization vectors, not to be confused with the Cartesian unit vectors,  $\hat{\mathbf{e}}_j$  ( $j=x,y,z$ ). We define a coordinate system local to the sheath:  $x$  denotes the direction normal to the sheath (with unit vector  $\mathbf{s} = \hat{\mathbf{e}}_x$  and sheath located at  $x = 0$ ) and  $(y, z)$  are the directions tangential to the sheath. In Eq. (5), we have assumed for simplicity that all waves have the same Fourier components in  $y$  and  $z$ , and Fourier analysis is possible because of the assumption of constant density in the vicinity of the wall. For each wave,  $k_x$  is determined numerically from  $k_y$  and  $k_z$  using the homogeneous plasma dispersion relation.

The wave polarization vectors  $\mathbf{e}_j$  are defined as follows in the limiting cases where approximate second-order dispersion relations are obtained.<sup>10,19</sup> Using the FW ordering  $n_{\perp}^2 \sim \varepsilon_{\perp}, \varepsilon_x \ll \varepsilon_{\parallel}$ , the wave polarization  $\mathbf{e}_{\text{FW}}$  is given by

$$\mathbf{e}_{\text{FW}} = C_{\text{FW}}(\mathbf{Q}\mathbf{n}_{\perp} + \mathbf{b} \times \mathbf{n}_{\perp}) , \quad \mathbf{Q} = \frac{-i\varepsilon_x}{(n_{\parallel}^2 - \varepsilon_{\perp})} . \quad (6)$$

For the SW ordering  $n_{\perp}^2 \sim \varepsilon_{\parallel} \gg \varepsilon_{\perp}, \varepsilon_x$ , the wave polarization  $\mathbf{e}_{\text{SW}}$  is given by

$$\mathbf{e}_{\text{SW}} = C_{\text{SW}}(\mathbf{G}\mathbf{n}_{\perp} + \mathbf{b}) , \quad \mathbf{G} = \frac{\mathbf{n}_{\parallel}}{(n_{\parallel}^2 - \varepsilon_{\perp})} , \quad (7)$$

where  $C_{\text{FW}}$  and  $C_{\text{SW}}$  are normalization constants. Note that  $\mathbf{b} \cdot \mathbf{e}_{\text{FW}} = 0$  and  $\mathbf{b} \cdot \mathbf{e}_{\text{SW}} \neq 0$ , so that the SW is required to obtain an  $E_{\parallel}$  component and generate an rf sheath potential.

Substituting Eq. (5) into Eq. (4), one obtains the following solution<sup>19</sup> for the field amplitudes of the reflected FW ( $E_1$ ) and evanescent SW ( $E_2$ ):

$$\frac{E_1}{E_0} = \frac{\mathbf{s} \cdot \mathbf{g}_2 \times \mathbf{g}_0}{\mathbf{s} \cdot \mathbf{g}_1 \times \mathbf{g}_2} \equiv \Theta , \quad \frac{E_2}{E_0} = \frac{\mathbf{s} \cdot \mathbf{g}_0 \times \mathbf{g}_1}{\mathbf{s} \cdot \mathbf{g}_1 \times \mathbf{g}_2} , \quad (8)$$

where  $E_0$  is the amplitude of the incident FW,

$$\mathbf{g}_j = \mathbf{e}_j - i \mathbf{k}_j \Delta (\mathbf{s} \cdot \boldsymbol{\varepsilon} \cdot \mathbf{e}_j) \quad (9)$$

and  $\mathbf{e}_j$  are the wave polarization vectors obtained from the homogeneous solution. Consistent with the ordering in Eq. (3), we assume  $k_x x \sim \delta_e / \delta_i \ll 1$  and neglect the exponential phase factors  $\sim \exp(ik_x x)$  for the FW. The first term in  $\mathbf{g}_j$  arises from the usual metal wall BC, and the second term is the sheath capacitance effect from the sheath BC term. Thus, the usual metal wall BC is still recovered when  $\Delta \rightarrow 0$ . Note that Eq. (8) has the property that the BC couples the FW ( $\mathbf{g}_0, \mathbf{g}_1$ ) to the SW ( $\mathbf{g}_2$ ). It was shown<sup>19</sup> that the resulting SW amplitude  $E_2$  is non-zero when the following three conditions are met: (i) there is a flux surface mismatch with the boundary ( $\mathbf{s} \cdot \mathbf{b} \neq 0$ ), as discussed above, (ii) the incident and reflected fast waves propagate in opposite directions, and (iii) the incident FW wavenumber  $\mathbf{k}$  has a component in the  $\mathbf{s} \times \mathbf{b}$  direction.

Combining Eqs. (5) and (8), we find that the total FW field is

$$\mathbf{E}_{\text{FW}} = E_0 \left( \mathbf{e}_0 e^{ik_0 x} + \mathbf{e}_1 \Theta e^{ik_1 x} \right), \quad (10)$$

where  $\Theta$  is the parameter defined in Eq. (8) and the dependence on  $\omega, k_y$  and  $k_z$  has been suppressed. In our previous work on far-field fast waves, the incident FW amplitude  $E_0$  was specified as an input to the sheath calculation, and Eq. (8) gave the solution for the other wave amplitudes. Here, the total FW field  $\mathbf{E}_{\text{FW}}$  is the fundamental quantity in formulating the boundary condition, so we need to invert Eq. (10) as follows

$$E_0 = \frac{-\mathbf{s} \cdot \mathbf{e}_1 \times \mathbf{E}_{\text{FW}}}{\mathbf{s} \cdot \mathbf{e}_0 \times \mathbf{e}_1}, \quad E_1 = \frac{\mathbf{s} \cdot \mathbf{e}_0 \times \mathbf{E}_{\text{FW}}}{\mathbf{s} \cdot \mathbf{e}_0 \times \mathbf{e}_1}. \quad (11)$$

The constraint on the individual amplitudes  $E_0$  and  $E_1$  is given by the first relation in Eq. (8), which can be rewritten as

$$\mathbf{s} \cdot \mathbf{g}_2 \times \mathbf{g}_0 E_0 - \mathbf{s} \cdot \mathbf{g}_1 \times \mathbf{g}_2 E_1 = 0. \quad (12)$$

The new ‘‘FW sheath BC’’ is obtained by combining Eqs. (11) and (12).

For electron-poor sheaths, obtained when  $(m_e / m_i)^{1/2} < \mathbf{s} \cdot \mathbf{b} < 1$ , Eqs. (11) and (12) combine to give the following BC

$$(\mathbf{s} \cdot \mathbf{g}_2 \times \mathbf{g}_0 \mathbf{s} \times \mathbf{e}_1 + \mathbf{s} \cdot \mathbf{g}_1 \times \mathbf{g}_2 \mathbf{s} \times \mathbf{e}_0) \cdot \mathbf{E}_{\text{FW}} = 0, \quad (13)$$



which imposes one scalar constraint on the total fast wave field,  $\mathbf{E}_{\text{FW}}$ . Using the substitution rule  $\mathbf{k} \rightarrow -i\nabla$  in Eq. (13), one obtains a relation among the spatial gradients of the FW field at the sheath-plasma boundary. This is the main result of the paper.

The SW physics enters the FW BC through the factors involving  $\mathbf{g}_2$ . Also, note that the normalization of the polarization vectors cancels out of the BC, because each term involves a triple product of the normalizations of the three polarization vectors ( $C_0 C_1 C_2 = C_{\text{FW}}^2 C_{\text{SW}}$ ). Finally, Eq. (4) shows that this BC reduces to the conducting wall BC when  $\Delta \rightarrow 0$ .

It is straightforward to calculate the rf sheath potential using this formalism, as discussed in Ref. 19. The steady-state (DC) sheath potential is

$$\Phi_{\text{sh}} \equiv C_{\text{sh}} \Phi_{\text{rf}} + 3T_e, \quad (14)$$

where the second term is the (approximate) Bohm sheath potential due to thermal electron loss,  $\Phi_{\text{rf}}$  is the rf sheath potential, and  $C_{\text{sh}} \Phi_{\text{rf}}$  is the “rectified” DC sheath potential ( $C_{\text{sh}}$  is an order unity rectification coefficient) with the conducting boundary assumed to be at zero potential. The rf sheath potential is obtained by summing over all waves, but typically the SW makes the dominant contribution:

$$\Phi_{\text{rf}} \equiv \Delta \left| \sum_{j=0}^2 \mathbf{s} \cdot \boldsymbol{\varepsilon}_j \cdot \mathbf{E}_j \right| \approx |\Delta \mathbf{s} \cdot \boldsymbol{\varepsilon} \cdot \mathbf{E}_2| \quad . \quad (15)$$

This can be seen as follows. When the B field mismatch factor  $\mathbf{s} \cdot \mathbf{b}$  is not too small, the electron terms involving  $\varepsilon_{\parallel}$  dominate the sum, viz.  $\mathbf{s} \cdot \boldsymbol{\varepsilon} \cdot \mathbf{E}_j \approx \mathbf{s} \cdot \mathbf{b} \varepsilon_{\parallel} \mathbf{b} \cdot \mathbf{E}_j = \mathbf{s} \cdot \mathbf{b} \varepsilon_{\parallel} \mathbf{b} \cdot \mathbf{E}_2$ . The last equality follows from the fact that the FW fields ( $\mathbf{E}_0, \mathbf{E}_1$ ) have no component parallel to  $\mathbf{B}$ . Thus, the SW  $E_{\parallel} = \mathbf{b} \cdot \mathbf{E}_2$  determines the magnitude of the rf sheath potential in the electron-dominated regime. In the present model,  $\mathbf{E}_2$  is given as a function of the fast wave field  $\mathbf{E}_{\text{FW}}$  by Eqs. (8) and (11).

In summary, we have derived a new BC for self-consistently calculating the rf fields and rf sheath potential at the wall during FW propagation [see Eq. (13)]. The BC is homogeneous in the FW field amplitude and reduces to the metal wall BC in the limit

$\Delta \rightarrow 0$  (vanishing sheath width). The BC is valid when the separation of scales in Eq. (3) applies. It contains the physics of coupling of a FW with  $E_{\parallel} = 0$  to a short scale length SW with  $E_{\parallel} \neq 0$ . This BC may be useful in rf wave propagation codes using finite-elements at the boundary (e.g. see Refs. 16-18) to allow studies of FW propagation without having to resolve the short SW scale numerically.

## **Acknowledgements**

The authors would like to thank Haruhiko Kohno for useful conversations. This work was supported by the U.S. Department of Energy (DOE) under DOE Grant Nos. DE-FG02-97ER54392 and DE-FC02-05ER54823; however, this support does not constitute an endorsement by the DOE of the views expressed herein.

## References

- <sup>1</sup> J.-M. Noterdaeme and G. Van Oost, *Plasma Phys. Control. Fusion* **35**, 1481 (1993).
- <sup>2</sup> J.R. Myra, D.A. D'Ippolito, D.A. Russell, L.A. Berry, E.F. Jaeger and M.D. Carter, *Nucl. Fusion* **46**, S455 (2006).
- <sup>3</sup> D.A. D'Ippolito and J.R. Myra, *J. Nucl. Mater.* **415**, S1001-S1004 (2011).
- <sup>4</sup> S.J. Wukitch, B. Lipschultz, E. Marmar, Y. Lin, A. Parisot, M. Reinke, J. Rice, J. Terry and C-Mod Team, *J. Nucl. Mater.* **363–365**, 491 (2007).
- <sup>5</sup> S. J. Wukitch, Y. Lin, B. LaBombard, B. Lipschultz, D. Whyte, and the Alcator C-Mod Team, *Proc. 22nd IAEA Fusion Energy Conf.* (Geneva, Switzerland, 2008) (IAEA, Vienna) paper IAEA-CN-165-EX/P6-23.
- <sup>6</sup> V. Bobkov, F. Braun, R. Dux, A. Herrmann, L. Giannone, A. Kallenbach, H. W. Müller, R. Neu, J.-M. Noterdaeme, T. Pütterich, V. Rohde, A. Sips, A. Krivska, I. Zammuto, and ASDEX Upgrade team, *Proc. 22nd IAEA Fusion Energy Conf.* (Geneva, Switzerland, 2008) (IAEA, Vienna) paper IAEA-CN-165-EX/P6-31.
- <sup>7</sup> V. Bobkov, F. Braun, L. Colas, R. Dux, H. Faugel, L. Giannone, A. Herrmann, A. Kallenbach, H. W. Müller, R. Neu, J.-M. Noterdaeme, Th. Pütterich, G. Siegl, E. Wolfrum, and ASDEX Upgrade Team, *J. Nucl. Mater.* **415**, S1005-S1008 (2011).
- <sup>8</sup> L. Colas, V. Basiuk, B. Beaumont, A. Bécoulet, G. Bosia, S. Brémond, M. Chantant, F. Clairet, A. Ekedahl, E. Faudot, A. Géraud, M. Goniche, S. Heuraux, G. T. Hoang, G. Lombard, L. Millon, R. Mitteau, P. Mollard, K. Vulliez, and the Tore Supra team, *Nucl. Fusion* **46**, S500 (2006).
- <sup>9</sup> L. Colas, Ph. Jacquet, G. Agarici, C. Portafaix, M. Goniche, and JET-EFDA contributors, *Proc. 18th Topical Conference on Radio Frequency Power in Plasmas*, Gent (AIP, New York, 2009), p. 133.
- <sup>10</sup> J.R. Myra, D.A. D'Ippolito and M. Bures, *Phys. Plasmas* **1**, 2890 (1994).
- <sup>11</sup> D.A. D'Ippolito and J.R. Myra, *Phys. Plasmas* **13**, 102508 (2006).
- <sup>12</sup> E.F. Jaeger, L.A. Berry, J.S. Tolliver, D.B. Batchelor, *Phys. Plasmas* **2**, 2597(1995).
- <sup>13</sup> C. D. Child, *Phys. Rev. (Series I)* **32**, 492 (1911); I. Langmuir, *Phys. Rev.* **21**, 419 (1923).

- <sup>14</sup> J.R. Myra and D.A. D’Ippolito, *Plasma Phys. Control. Fusion* **52**, 015003 (2010).
- <sup>15</sup> D. A. D’Ippolito and J. R. Myra, *Phys. Plasmas* **17**, 072508 (2010).
- <sup>16</sup> H. Kohno, *Numerical analysis of radio-frequency sheath-plasma interactions in the ion cyclotron range of frequencies*, Sc.D. thesis, MIT (2011).
- <sup>17</sup> “A finite element procedure for radio-frequency sheath-plasma interactions in the ion cyclotron range of frequencies,” H. Kohno, J. R. Myra, and D. A. D’Ippolito, submitted to *Comput. Phys. Commun.* (2011).
- <sup>18</sup> “Numerical analysis of radio-frequency sheath-plasma interactions in the ion cyclotron range of frequencies,” H. Kohno, J. R. Myra, and D. A. D’Ippolito, submitted to *Phys. Plasmas* (2011).
- <sup>19</sup> D. A. D’Ippolito, J. R. Myra, E. F. Jaeger, and L. A. Berry, *Phys. Plasmas* **15**, 102501 (2008).
- <sup>20</sup> F. W. Perkins, *Bull. Am. Phys. Soc.* **34**, 2093 (1989), paper 6S6.
- <sup>21</sup> M. Brambilla, R. Chodura, J. Hoffmann, and J. Neuhauser, in *Plasma Phys. Control. Nucl. Fusion Res. 1990 (IAEA, Vienna, 1991)*, Vol. 1, p. 723.
- <sup>22</sup> S.J. Wukitch, B. LaBombard, Y. Lin, B. Lipschultz, E. Marmor, M.L. Reinke, D.G. Whyte, and the Alcator C-Mod Team, *J. Nucl. Mater.*, **390-391**, 951 (2009).
- <sup>23</sup> J. Hosea, R. E. Bell, B. P. LeBlanc, C. K. Phillips, G. Taylor, E. Valeo, J. R. Wilson, E. F. Jaeger, P. M. Ryan, J. Wilgen, H. Yuh, F. Levinton, S. Sabbagh, K. Tritz, J. Parker, P. T. Bonoli, R. Harvey, and NSTX Team, *Phys. Plasmas* **15**, 056104 (2008).
- <sup>24</sup> P. M. Ryan, R. E. Bell, L. A. Berry, P. T. Bonoli, R. W. Harvey, J. C. Hosea, E. F. Jaeger, B. P. LeBlanc, C. K. Phillips, G. Taylor, E. J. Valeo, J. B. Wilgen, J. R. Wilson, J. C. Wright, H. Yuh, and the NSTX Team, *Proceedings of the 35th EPS Conference on Plasma Phys.*, Hersonissos, Greece, 9 - 13 June, 2008, ECA Vol.32, P-1.108 (2008)